A Modular Approach for the Optogenetic Control of Small GTPase Activity in Living Cells

Benjamin Faulkner,[1] Yuchen He,[1] Daniel Sitrin,[1] Linda Ziamanesh,[1] and Cliff I. Stains[1,2,3]*

[1]Department of Chemistry, University of Virginia, Charlottesville, VA 22904, USA

[2]University of Virginia Cancer Center, University of Virginia, Charlottesville, VA 22904, USA

[3]Virginia Drug Discovery Consortium, Blacksburg, VA 24061, USA

*Corresponding author, E-mail: cstains@virginia.edu

Abstract

Small GTPases are critical regulators of cellular processes, such as cell migration, and comprise a family of over 167 proteins in the human genome. Despite the essential role these proteins play in maintaining cell homeostasis, there is no generalizable method for directly controlling the activity of these signaling enzymes with subcellular precision. Herein, we report the design and implementation of a modular, optogenetic platform for the spatial control of small GTPase activity within living cells. By combining split-small GTPases with improved Light-Inducible Dimerization (iLID) domains, we obtain spLIT-small GTPase constructs that enable spatially precise control of cytoskeletal dynamics such as filopodia formation (spLIT-Cdc42), membrane retraction (spLIT-RhoA), and directed cell migration (spLIT-Rac1). These results establish spLIT-small GTPases as a modular optogenetic platform for spatially controlled activation of small GTPase signaling within living cells and demonstrate the ability to probe spatiotemporal aspects of cell signaling using this approach.

Introduction

Small GTPases represent a diverse family of protein switches in mammalian cells and play pivotal roles in regulating a variety of essential cellular processes including cell survival, cell morphology, vesicle trafficking, and cell movement.[1-4] In normal physiology, the activity of small GTPases is regulated via cycling between a guanosine triphosphate (GTP)-bound active state and a guanosine diphosphate (GDP)-bound inactive state (**Figure 1a**).[5] This cycle of activation and inactivation is mainly regulated by two regulatory proteins: guanine nucleotide exchange factors (GEFs), which facilitate the exchange of GDP for GTP, and GTPase-activating proteins (GAPs), which accelerate the hydrolysis of GTP to GDP.[6] Furthermore, a lipidation sequence present at either the N- or C-terminus of a small GTPases can influence localization within a cell.[7,8] Given their essential roles in cellular processes, mutations that perturb small GTPase regulation contribute to a range of diseases including cancer,[9,10] neurodegenerative diseases,[11-13] cardiovascular diseases,[14-16] and immune disorders.[17-19] Additionally, the redistribution of small GTPase activity within a cell upon treatment with chemotherapeutics has been shown to confer drug resistance.[20,21] As such, understanding the molecular mechanisms that govern small GTPase activity at the subcellular level and developing tools to modulate their function with spatial precision remains a critical goal in biomedical research.

Since the discovery of the Rat sarcoma (Ras) oncogene in the early 1980s,[22] efforts to develop small molecule inhibitors to regulate small GTPase activity have persisted. However, these efforts have faced significant challenges due to the strong affinity of small GTPases for their natural substrates and an apparent lack of accessible allosteric binding pockets.[23] Progress has been made recently in targeting small GTPases through covalent modification of residues near the GTP-binding site, a strategy that has since led to the first generation of small GTPase inhibitors entering the clinic.[24-29] Nonetheless, this approach lacks the spatial resolution required to dissect the influence of subcellularly localized small GTPase activity. As a result, protein

engineering-based approaches have gained increased attention for their ability to offer more precise, spatiotemporally controlled activation of small GTPase activity.[30-33]

Hahn and colleagues demonstrated the ability to control the activity of the small GTPase Rac1 by fusing a light, oxygen, or voltage (LOV) domain near the effector binding site of a constitutively active Rac1 mutant, rendering it inactive until exposure to blue light (450 nm – 500 nm).[34] This light-activated system offers high temporal and spatial resolution for controlling small GTPase activity in living cells. Although, its reliance on a noncovalent binding interface between the LOV domain and Rac1 poses challenges for broad application across the small GTPase family, requiring intensive case-by-case optimization for each small GTPase. For example, when used to control the activity of the closely related small GTPase Cdc42, mutations had to be made in Cdc42 to obtain proper occlusion of its effector binding site in the dark state.[34] Development of an alternative approach utilizing protein sequestration to localize GEFs to the inner cell membrane, LOVTRAP, allowed for a more generalizable approach to control the activity of other membrane-localized small GTPases such as RhoA and Rac1.[35] Subsequently, Toettcher and colleagues developed the OptoSOS system to spatially regulate the activity of a RasGEF, SOS, via the selective localization of the GEF to the cell membrane using a light-responsive dimerization system.[36,37] This method proved effective to study ERK signaling dynamics involved in cell prolioferation.[37,38] Although powerful, the cross-reactivity of GEFs with multiple small GTPases can complicate analysis of individual small GTPase outputs within complex cellular circuits.

We have previously described a standardized part set for the plug-and-play activation of small GTPases using chemical-inducible dimerization (CID) domains.[39,40] By leveraging the high sequence and structural homology among small GTPases, we applied a fragmentation site originally identified in Cdc42[41] to other small GTPases across the superfamily, including Rac1, RhoA, and KRas, without the need for optimization (**Figure 1b**). Fusion of the relevant split-small

GTPase fragments to CID domains enabled the small molecule-driven reassembly of each small GTPase, allowing for temporal control of small GTPase activity in living cells. While this approach allows for the potential dissection of small GTPase signaling within living cells, certain applications can suffer from the lack of spatial resolution and off-target effects arising from the use of CIDs to control split-small GTPase reassembly. Herein, we sought to enable subcellular activation of small GTPase signaling through optogenetically-controlled reassembly of split-small GTPases (**Figure 1c**). The resulting platform enables localized activation of small GTPase signaling with high spatiotemporal resolution and can be paired with the appropriate split-small GTPase to modulate a chosen cellular phenotype. Additionally, we demonstrate that the extent of signaling activation in this system can be rationally tuned. In the long term, we envision that our approach will enable spatial regulation of signaling within living cells, advancing applications in biomedical research and synthetic biology.

Results and Discussion

Light-Gated Activation of spLIT-Cdc42

The last 20 years have seen a substantial rise in the field of optogenetics with the discovery and development of light-responsive protein domains that can be genetically incorporated into host cells.[42] By coupling proteins-of-interest to these light-responsive protein domains, native cellular processes can be studied with greater spatial precision or reengineered to generate novel cellular functions.[43-49] Numerous light-responsive protein domains have since been discovered with excitation wavelengths ranging from the ultraviolet (~300 nm) to the near-infrared (>750 nm).[50-56] To pair with our split-small GTPase fragments in mammalian cells, we chose the improved light-inducible dimerization, iLID, system given the orthogonality of its protein domains to mammalian cells and native chromophore, flavin mononucleotide (FMN).[57] Additionally, the availability of multiple variants of the iLID system, each with their own unique binding affinities in the lit and dark states, should allow for the tunability of small GTPase activity in cells.[57,58] The iLID system utilizes the light, oxygen, or voltage 2 (LOV2) domain of phototropin 1 from *Avena sativa*.[59] Upon exposure to blue light (450 nm – 500 nm) the LOV2 domain undergoes conformational changes by forming a temporary covalent bond between a reactive cysteine residue within the core of the LOV2 protein and FMN. These conformational changes result in the eventual dissociation and unwinding of a C-terminal α-helix, commonly referred to as the Jα-helix. In iLID, the Jα-helix has a short SsrA peptide tag incorporated into its C-terminal end that conditionally binds to its binding partner, SspB, upon blue-light exposure and subsequent uncaging from the core of the LOV2 protein domain. We hypothesized that fusion of our N-terminal and C-terminal split-small GTPase fragments to SspB and iLID, respectively, would allow for the conditional localization and reassembly of small GTPase fragments upon activation with blue light.

To investigate our hypothesis, we designed light-gated split-Cdc42 (spLIT-Cdc42) constructs by fusing the N-terminal fragment of a constitutively active mutant of Cdc42 (Q61L) to

the C-terminus of SspB and the C-terminal fragment to the N-terminus of iLID (**Figure S1**). To monitor expression of our proteins in cells, we fused a red-fluorescent protein to the N-terminus of SspB and a yellow fluorescent protein to the C-terminus of iLID followed by a CAAX box for localization to the cytosolic face of the membrane. Both fragments were subsequently cloned into a vector containing an internal ribosome entry site to allow for bicistronic expression (**Figure S1**, **Tables S1**, and **S2**). To explore the tunability of Cdc42 activation, we fused the N-terminal fragment of Cdc42 to the Nano, Milli, and Micro mutants of SspB,[57,58] yielding three distinct constructs with different binding affinities in the lit and dark state (**Figure S1**).

A well-established, canonical role of Cdc42 signaling in mammalian cells is the induction of filopodia formation.[60] Filopodia are long, filamentous protrusions from the cell membrane that serve diverse functions in cell movement and intercellular communication.[61] To first verify the activity of spLIT-Cdc42 in cells, we sought to reproduce previous findings utilizing a rapamycin-gated split-Cdc42 design by globally illuminating cells with blue light (**Figure 2a**).[39] As a negative control, nontransfected HeLa cells exposed to global illumination with blue light for 30 minutes showed no significant change in filopodia density before or after exposure to light (**Figure 2b** and **f**). To test our spLIT-Cdc42 constructs, we began with the highest affinity mutant, spLIT-Cdc42-Nano, to increase the likelihood of detecting changes in filopodia density. Transiently transfected HeLa cells were exposed to blue light, imaged (**Figures 2c, S2a**), and filopodia formation was quantified demonstrating a 2.9-fold increase in filopodia density after exposure as compared to pre-exposure levels (**Figure 2f**). Importantly, only cells expressing both the N- and C-terminal fragments, as by imaging the fluorescent protein tags (**Figure S2**), were used in quantification. As an additional control, we mutated the reactive cysteine residue within the LOV2 domain of iLID to an alanine, abolishing the formation of the covalent bond between iLID and FMN upon stimulation with blue light. As expected, illumination of HeLa cells expressing spLIT-Cdc42-Nano-C252A did not lead to an increase in filopodia density of the cells (**Figures 2c, 2f, S2b**). To explore

the tunability of spLIT-Cdc42, we then tested the two additional variants of SspB, Micro and Milli. Cells expressing spLIT-Cdc42-Micro exhibited a 2.1-fold increase in filopodia density after illumination (**Figures 2d, 2f, S2c**), albeit with a lower absolute filopodia density compared to cells expressing spLIT-Cdc42-Nano. No change in filopodia density was observed for SspB-Milli, indicating that the lit-state affinity of this iLID system was too weak to drive signaling from the Cdc42 fragments (**Figures 2e, 2f, S2e**). Mutation of the reactive cysteine in spLIT-Cdc42-Micro-C252A and spLIT-Cdc42-Milli-C252A eliminated any change in filopodia density in transfected cells (**Figures 2d-f**). Taken together, these results clearly indicate that spLIT-Cdc42 can optically control Cdc42 activity in mammalian cells with tunable outputs.

Spatial Regulation of Filopodia Formation

We next sought to demonstrate the spatial precision of spLIT-Cdc42 by illuminating only a small subsection of cell membrane. Using this approach, only the protein fragments within the area of exposure should reassemble, leading to a localized cellular response (**Figure 3a**). We began by illuminating one end of a cell expressing spLIT-Cdc42-Nano as verified before light exposure by imaging fluorescent protein tags (**Figures 3b-c, S3a**). The change in filopodia density before and after exposure within the illuminated region of the cell (blue square) was then normalized to the change in filopodia density of a nonilluminated region on the opposite end of the cell (gray square). Upon comparison, the illuminated region exhibited a 2.6-fold increase in filopodia density relative to the nonilluminated region (**Figure 3h**). Repeating the experiment with cells expressing the spLIT-Cdc42-Nano-C252A mutant (**Figures 3b, 3d, S3b**) resulted in no change in filopodia formation (**Figure 3h**). A similar outcome was observed in cells expressing spLIT-Cdc42-Micro (**Figures 3e-f, S3c**) and spLIT-Cdc42-Micro-C252A (**Figures 3e, 3g, S3d**) with a relative fold change in filopodia density of 1.4 for spLIT-Cdc42-Micro (**Figure 3h**). These results highlight the ability to spatially control Cdc42 activation using this system and indicate the ability to tune Cdc42 signaling by utilizing iLID systems with varying affinities. Although cells

expressing the spLIT-Cdc42-Nano system exhibited higher formation of filopodia when exposed to blue light than those expressing spLIT-Cdc42-Micro, cells expressing the spLIT-Cdc42-Nano system also had a higher level of filopodia formation prior to exposure (**Figure 2f**). Therefore, we chose to proceed with the SspB-Micro iLID system in subsequent experiments since the reduced affinity of these components appeared to decrease split-small GTPase reassembly in the dark state while still enabling an observable change in cellular phenotype in the lit state.

RhoA-Induced Membrane Retraction

The Rho subfamily of small GTPases, to which Cdc42 belongs, currently contains 20 unique members.[62] To investigate the modular nature of our optogenetic spLIT-Cdc42 system, we set out to develop spLIT-GTPase constructs for additional Rho family members. RhoA functions as a molecular switch in the regulation of downstream effectors such as Rho-associated kinase (ROCK) and mDia1, leading to actomyosin contractility, stress fiber formation, and focal adhesion assembly.[63] These processes contribute to large-scale contraction of the cell membrane, allowing for force generation and directional cell movement. We previously demonstrated that CIDs could be used to gate split-RhoA-mediated cell membrane retraction on a global scale within cells.[39,40] We hypothesized that replacing the Cdc42 fragments within spLIT-Cdc42 with the corresponding RhoA fragments would enable the spatial regulation of cell membrane contraction using light (**Figure 4a**). Accordingly, we replaced the Cdc42 fragments of spLIT-Cdc42-Micro and spLIT-Cdc42-Micro-C252A with the corresponding fragments of RhoA, generating spLIT-RhoA-Micro and spLIT-RhoA-Micro-C252A, respectively (**Figure S1**, **Tables S1**, and **S2**). Spatially restricted illumination of cells expressing spLIT-RhoA-Micro (**Figures 4b**, **S4a**, and **Video S1**) led to a 2-fold increase in retraction compared to cells expressing spLIT-RhoA-Micro-C252A (**Figures 4c-d**, **S4b**, and **Video S2**), indicating the ability to activate RhoA signaling with light. Interestingly, activation of spLIT-RhoA-Micro consistently led to an equivalent decrease in cell area in both the exposed and control regions of cells (**Figures 4b**). However, a large decrease in cell area in either

the exposed or control regions of cells expressing spLIT-RhoA-Micro-C252A was not observed (**Figure 4c**). Since the retraction of the cell membrane in the control region was equivalent in magnitude to the exposed region for spLIT-RhoA-Micro expressing cells, the observed decrease in cell area in the exposed region (**Figure 4d**) was comparable to the global decrease in cell area (2.6-fold higher for cells expressing spLIT-RhoA-Micro [**Figure 4e**]). Importantly, a pronounced decrease in cell area was not observed in either exposed or control regions of spLIT-RhoA-Micro-C252A expressing cells (**Figures 4c**, **d**, and **e**), indicating that increased cell retraction observed in spLIT-RhoA-Micro expressing cells was due to RhoA activation rather than stimulation with light.

We hypothesize that the bipolar cellular retraction observed upon localized activation of spLIT-RhoA-Micro could be a consequence of endogenous Rho GTPase signaling. Evidence suggests that localized RhoA activation can perpetuate to distal regions of the cell, possibly through the diffusion of RhoA effectors, such as ROCK, and through the inherent feed-forward control of RhoA activity.[64,65] This effect could cause the localized activation of RhoA within a cell to extend beyond the region exposed to light in our system, leading to bipolar membrane retraction. Additionally, it has been reported that knockdown of RhoA activity in human cancer cells leads to simultaneous lateral expansion of the cell membrane at opposing ends of the cell,[66] the opposite phenotype that we observe here for localized activation of spLIT-RhoA (**Figure 4b**). Thus, our results support the ability of localized RhoA signaling to perpetuate to distant regions of the cell. These results also highlight the ability to identify phenotypes arising from spatially localized activation using spLIT-RhoA. Ongoing efforts in our lab are focused on dissecting spatially localized RhoA activation and its ability to influence phenotypes at distant areas in the cell.

Optogenetic Control of Cell Movement

Rac1, another member of the Rho subfamily of small GTPases, regulates the formation of lamellipodia through its effectors, p-21 activating kinase (PAK) and WASP-family verprolin homologous protein (WAVE).[67] Physiologically, Rac1 aids in the outward projection of the cell membrane, allowing the cell to move forward. We hypothesized that local activation of spLIT-Rac1 could lead to directional control of cell movement (**Figure 5a**). To test whether we could bias the direction of movement of living cells, we cloned spLIT-Rac1-Micro and spLIT-Rac1-Micro-C252A (**Figure S1**, **Tables S1**, and **S2**). Excitingly, spatially restricted exposure of MEF cells expressing spLIT-Rac1-Micro to light led to clear cell membrane protrusion in the direction of light exposure (**Figures 5b, S5a, Videos S3-S6**). Additionally, we observed membrane retraction on the opposing end of the cell, leading to observable cell motion in the direction of light exposure. Conversely, cells expressing the spLIT-Rac1-Micro-C252A mutant did not respond to light stimulation (**Figures 5c, S5b, Videos S7-S11**). Since cells expressing the spLIT-Rac1-Micro construct did not move at a consistent rate from cell-to-cell, we sought to quantify movement across multiple cells using an index-based approach. In short, individuals with varying levels of familiarity with the experiment rated the directional movement of each cell relative to an arbitrary red dot posted on a video of each cell (**Figure 5d**). Importantly, raters were unaware of which protein construct each cell expressed nor the position of light exposure. Aggregated ratings revealed a clear trend: cells expressing spLIT-Rac1-Micro predominately moved towards the direction of light exposure while cells expressing spLIT-Rac1-Micro-C252A exhibited slight retraction away from the light stimulus (**Figure 5e**). These data indicate the ability to control the direction of cell movement using spLIT-Rac1-Micro. Although binding of the iLID system is rapidly reversible,[57,58,68] it remains unclear whether spLIT-Rac1 reassembly is reversable. Our lab is currently investigating the reversibility of our spLIT-Rac1 constructs (as well as other split-small GTPases) and whether sustained illumination could further impact cell movement.

Conclusion

In summary, we present the development and application of a modular, optogenetic system to control the activity of small GTPases in living cells. Leveraging light-inducible dimerization of the iLID system, we successfully reconstituted split-protein fragments corresponding to constitutively active Cdc42, RhoA, and Rac1, enabling subcellular control of key cellular processes such as filopodia formation, membrane retraction, and directional cell movement. Our results highlight the specificity, modularity, tunability, and spatially restricted nature of this light-induced split-small GTPase activation system.

Prolonged exposure to blue light can lead to DNA damage and induction of apoptosis in cells. As such, utilizing blue light to control protein activity may cause off-target effects that could impact results in certain applications, such as the study of apoptotic signaling pathways. To combat this issue, we limited exposure to blue-light exposure to short, non-continuous bursts. Looking ahead, the spLIT-small GTPase system offers a powerful tool to explore the spatial regulation of small GTPase signaling, such as bipolar membrane retraction induced by localized RhoA activation, as discussed above. Pairing our blue-light responsive spLIT-small GTPase constructs with split-small GTPases under the control of a spectrally orthogonal light-induced dimerization domains[50-56] could potentially allow for multiplexed experiments, elucidating potential crosstalk between small GTPase signaling pathways. Taken together, we believe that the technology described here will find broad applications in studying fundamental aspects of small GTPase signaling and in synthetic biology efforts to engineer new functions into living systems.

Supporting Information

Supporting Figures, Tables, Video Captions, and Instrumentation and Methods.

Acknowledgements

We thank the W.M. Keck Center for Cellular Imaging for the usage of the Leica STELLARIS 8 confocal/FLIM/tauSTED microscope system (NIH OD030409) and members of the C. Stains lab for editing the manuscript and helpful conversations. We acknowledge financial support from the NIH (R35GM148221) and the University of Virginia. The content of this work is solely the responsibility of the authors and does not necessarily represent the official views of the NIH.

Conflicts of Interest

B.F., Y.H., and C.I.S. have filed a patent covering split-small GTPases.

Figure 1

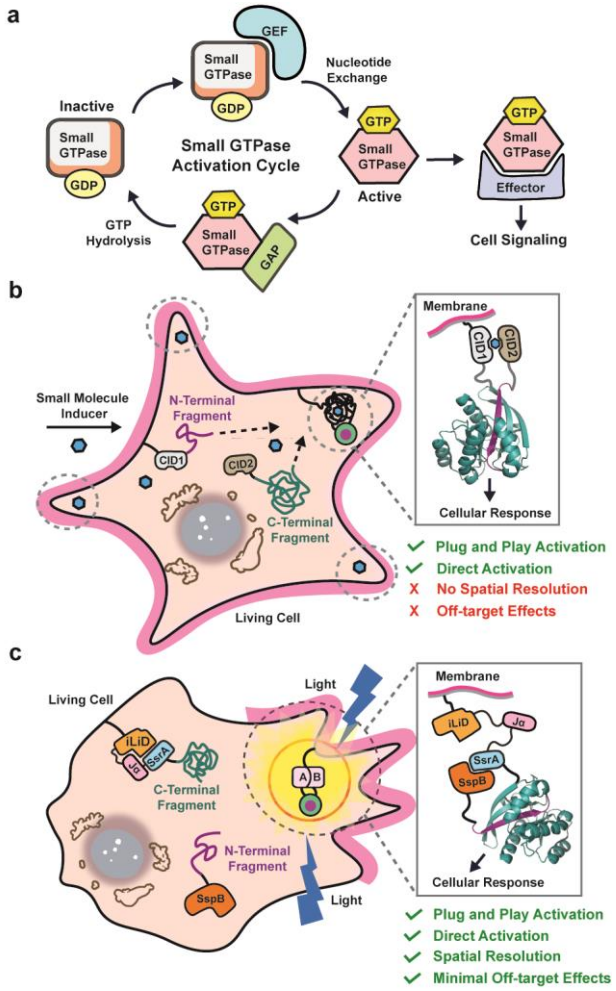

Split-protein engineering approaches to control small GTPase activity. (a) Schematic illustrating the regulatory cycle of small GTPase activity. (b) Fusion of small GTPase fragments to CID domains allows for the conditional reassembly and activation of small GTPases with user-defined inputs. (c) Replacing the CID domains with the iLID system allows for spatial resolution of split-small GTPase activation.

Figure 2

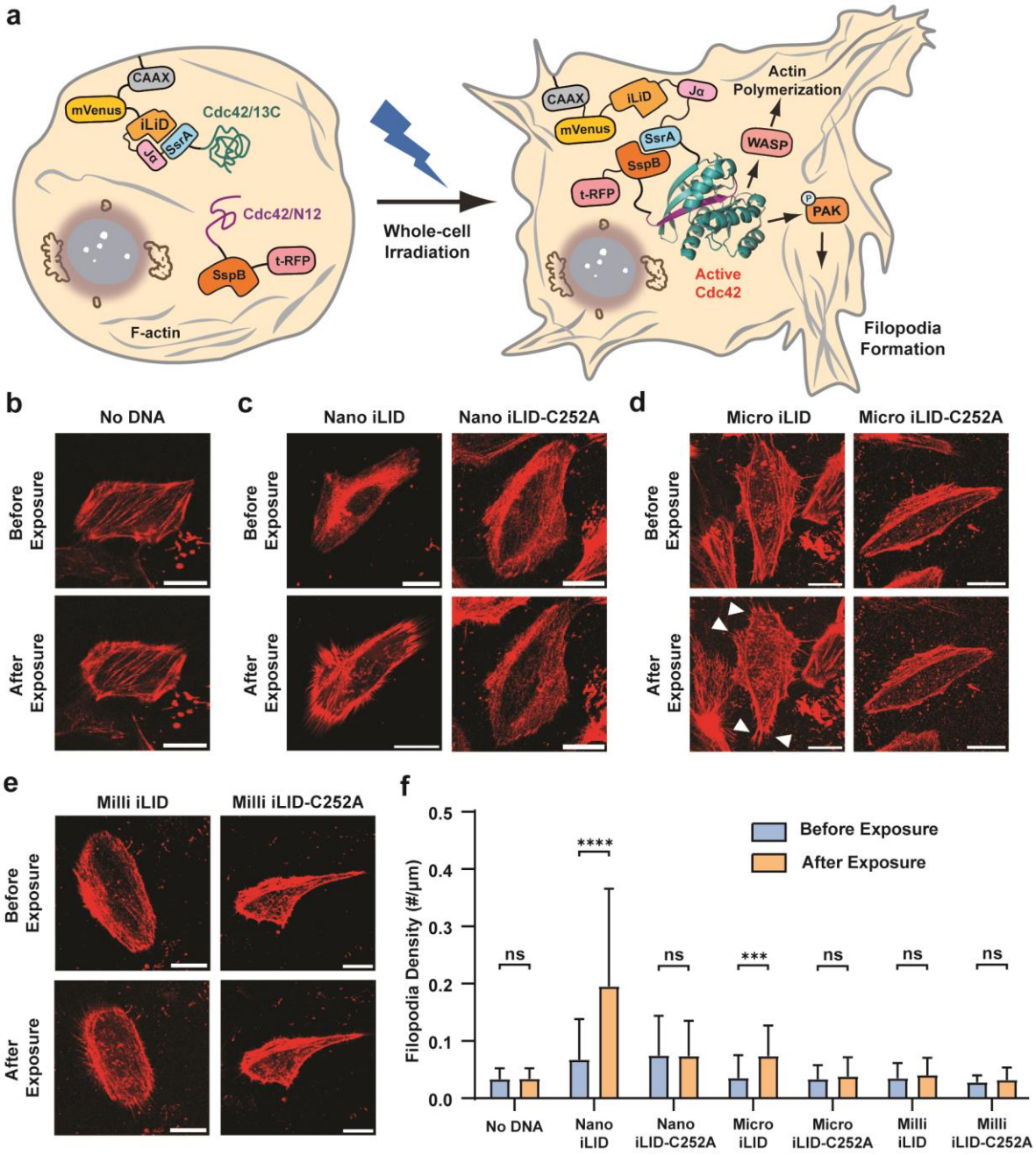

Regulating the formation of filopodia in living cells using spLIT-Cdc42. (a) Schematic illustrating the whole-cell irradiation of living cells to reassemble spLIT-Cdc42 and induce cell-wide filopodia formation. (b-e) Representative confocal images (F-actin stain channel shown) before and after whole-cell irradiation of (b) nontransfected HeLa cells, (c) HeLa cells expressing the spLIT-Cdc42-Nano systems, (d) HeLa cells expressing the spLIT-Cdc42-Micro systems, and (e) HeLa cells expressing the spLIT-Cdc42-Milli systems. Verification of spLIT-Cdc42 fragment expression can be found in **Figure S2** for each cell shown. (f) Quantification of filopodia density (number of filopodia divided by cell edge length) before and after global irradiation using FiloQuant.[69] Data

for each construct represents the average of at least 30 cells from at least 2 biological replicates. Statistical significance was determined using a two-tailed, unpaired Student's *t*-test. Error bars represent the standard deviation of the mean. All scale bars represent 20 μm. **** indicates a p-value of <0.0001, *** indicates a p-value of <0.001, and ns indicates a p-value of >0.05. Cells were simultaneously stimulated using 480 nm and 488 nm lasers at 20% intensity (50-55 μW) for 5 minutes followed by a 5-minute rest period in the dark. This was repeated for a total of 30 minutes.

Figure 3

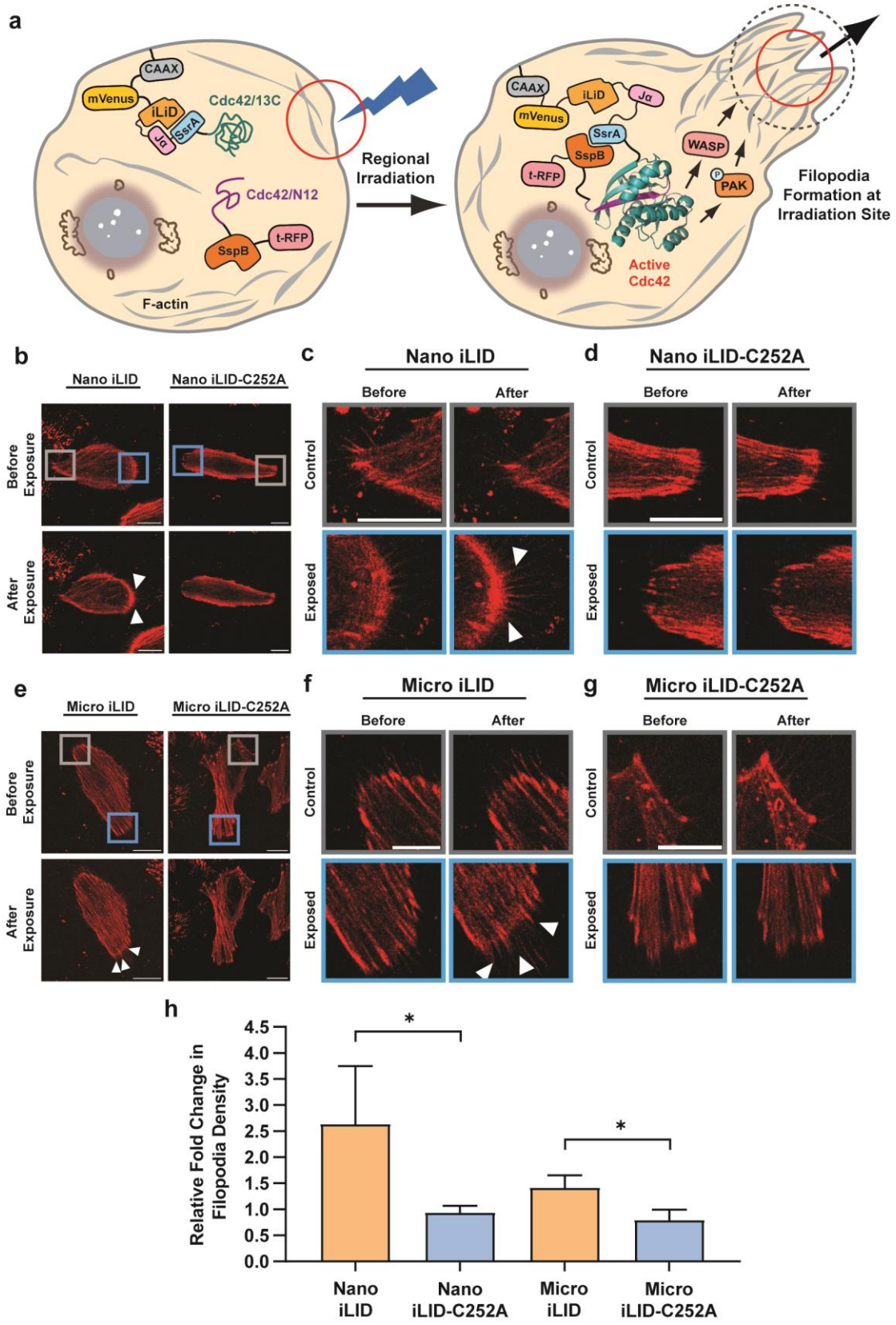
a
CAAX
mVenus
iLiD
Jα
SsrA
Cdc42/13C
Cdc42/N12
SspB
t-RFP
F-actin
Regional Irradiation
WASP
PAK
Active Cdc42
Filopodia Formation at Irradiation Site
b
Nano iLID
Nano iLID-C252A
Before Exposure
After Exposure
c
Nano iLID
Before
After
Control
Exposed
d
Nano iLID-C252A
e
Micro iLID
Micro iLID-C252A
f
Micro iLID
g
Micro iLID-C252A
h
Relative Fold Change in Filopodia Density
4.5
4.0
3.5
3.0
2.5
2.0
1.5
1.0
0.5
0.0
*
Nano iLID
Nano iLID-C252A
Micro iLID
Micro iLID-C252A

Spatially controlled filopodia formation. (a) Schematic illustrating the spatially confined activation of filopodia formation via the subcellular activation of spLIT-Cdc42 in living cells. (b) Representative confocal images (F-actin stain channel shown) of HeLa cells expressing the spLIT-Cdc42-Nano systems before and after site-specific irradiation. Verification of spLIT-Cdc42 fragment expression can be found in **Figure S3** for each cell shown. (c) Magnified images of the exposed region (blue square) and control region (grey square) of the cell expressing spLIT-Cdc42-Nano from panel (b). (d) Magnified images of the exposed region (blue square) and control region (grey square) of the cell expressing spLIT-Cdc42-Nano-C252A from panel (b). (e) Representative confocal images (F-actin stain channel shown) of HeLa cells expressing the spLIT-Cdc42-Micro systems before and after site-specific irradiation. Verification of spLIT-Cdc42 fragment expression can be found in **Figure S3** for each cell shown. (f) Magnified images of the exposed region (blue square) and control region (grey square) of the cell expressing spLIT-Cdc42-Micro from panel (e). (g) Magnified images of the exposed region (blue square) and control region (grey square) of the cell expressing spLIT-Cdc42-Micro-C252A from panel (e). (h) Quantification of the fold-change in filopodia formation before and after irradiation of the exposed end of the cells relative to the nonexposed end of the cells. Data for each construct represents the average of at least 3 cells from independent biological replicates. Statistical significance was determined using a two-tailed, unpaired Student's *t*-test. Error bars represent standard deviation of the mean. All scale bars represent 20 μm. * indicates a p-value of <0.05. Cells were stimulated using a 480 nm laser at 1-3% intensity (10-15 μW) for 30 seconds followed by a 30-second rest period in the dark. This was repeated for a total of 10 minutes.

Figure 4

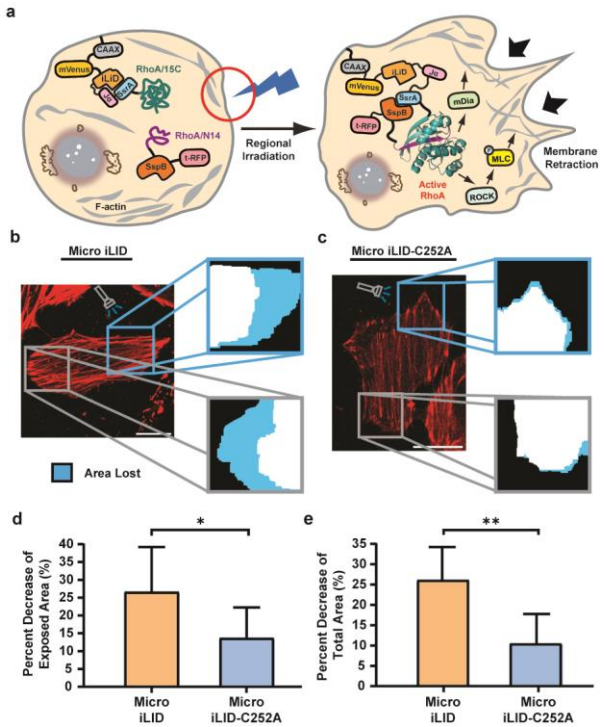

Localized activation of spLIT-RhoA leads to bipolar cell retraction. (a) Schematic illustrating the spatially confined activation of spLIT-RhoA in living cells. (b) Representative confocal image (F-actin stain channel shown) of a HeLa cell expressing spLIT-RhoA-Micro and exposed to light on one side (blue square). Verification of spLIT-RhoA fragment expression can be found in **Figure S4a** for the cell shown. Zoomed in images illustrate the reduction in cell area post exposure within the exposed region (blue square) and control region (grey square). (c) Representative confocal image (F-actin stain channel shown) of a HeLa cell expressing spLIT-RhoA-Micro-C252A and exposed to light on one side (blue square). Verification of spLIT-RhoA fragment expression can be found in **Figure S4b** for the cell shown. Zoomed in images illustrate the cell area reduction post exposure within the exposed region (blue square) and control region (grey square). (d) Quantification of the reduction in cell area within the exposed region for cells expressing spLIT-RhoA-Micro and spLIT-RhoA-Micro-C252A. Data for each construct represents the average of at least 6 cells from at least 5 independent biological replicates. (e) Quantification of the decrease in total area of the same cells expressing spLIT-RhoA-Micro (n=6) or spLIT-RhoA-Micro-C252A (n=9) post irradiation from panel (d). HeLa cells expressing the active spLIT-RhoA-Micro system exhibit a larger decrease in total cell area post irradiation. Statistical significance was determined using a two-tailed, unpaired Student's *t*-test. Error bars represent standard deviation of the mean. All scale bars represent 20 μm. * indicates a p-value of <0.05. Cells were stimulated using a 480 nm laser at 1-3% intensity (10-15 μW) for 30 seconds followed by a 30-second rest period in the dark. This was repeated for a total of 10 minutes.

Figure 5

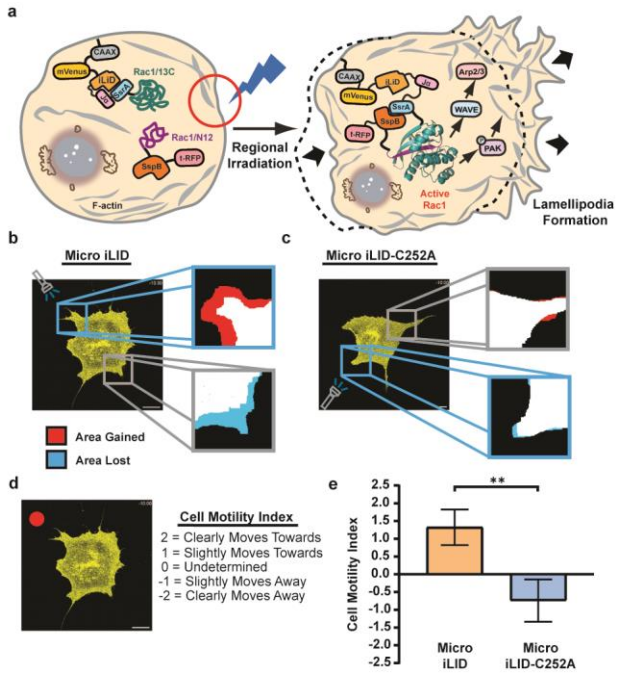

Controlling directional cell movement via spatially restricted Rac1 activation. (a) Schematic illustrating the spatial regulation of lamellipodia formation via the subcellular activation of spLIT-Rac1 in living cells. (b) Representative confocal image (mVenus channel shown) of a MEF cell expressing spLIT-Rac1-Micro and selectively exposed to light. Verification of spLIT-Rac1 fragment expression can be found in **Figure S5a**. Zoomed in images illustrate the change in cell area post exposure within the exposed region (blue square) and control region (grey square). (c) Representative confocal image (mVenus channel shown) of a MEF cell expressing spLIT-Rac1-Micro-C252A and selectively exposed to light. Verification of spLIT-Rac1 fragment expression can be found in **Figure S5b**. Zoomed in images illustrate the change in cell area post exposure within the exposed region (blue square) and control region (grey square). (d) Left - Representative image of a video given to raters. The red dot is a reference point. Right - Raters were tasked with choosing one of the “Cell Motility Index” rankings for each cell. (e) Quantification of cell motility for MEF cells expressing spLIT-Rac1-Micro (n=4) and spLIT-Rac1-Micro-C252A (n=5). Each cell is from an independent biological replicate. Data was aggregated from 13 independent, blinded ratings for each cell. Statistical significance was determined using a two-tailed, unpaired Student's *t*-test. Error bars represent standard deviation of the mean. All scale bars represent 20 μm. ** indicates a p-value of <0.01. Cells were stimulated using a 480 nm laser at 1-3% intensity (10-15 μW) for 30 seconds followed by a 30-second rest period in the dark. This was repeated for a total of 10 minutes.

Table of Contents Figure

Modular, Light-Gated Activation of Small GTPase Signaling

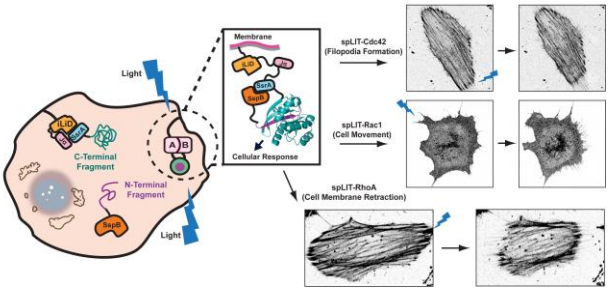

References

(1) Bourne, H. R.; Sanders, D. A.; McCormick, F. The GTPase superfamily: a conserved switch for diverse cell functions. *Nature* **1990**, *348* (6297), 125-132.
(2) Stryer, L.; Bourne, H. R. G proteins: a family of signal transducers. *Annu. Rev. Cell Dev. Biol.* **1986**, *2*, 391-419.
(3) Cherfils, J.; Zeghouf, M. Regulation of small GTPases by GEFs, GAPs, and GDIs. *Physiol. Rev.* **2013**, *93* (1), 269-309.
(4) Yin, G.; Huang, J.; Petela, J.; Jiang, H.; Zhang, Y.; Gong, S.; Wu, J.; Liu, B.; Shi, J.; Gao, Y. Targeting small GTPases: emerging grasps on previously untamable targets, pioneered by KRAS. *Signal Transduct. Target. Ther.* **2023**, *8* (1), 212.
(5) Cromm, P. M.; Spiegel, J.; Grossmann, T. N.; Waldmann, H. Direct Modulation of Small GTPase Activity and Function. *Angew. Chem. Int. Ed.* **2015**, *54* (46), 13516-13537.
(6) Bos, J. L.; Rehmann, H.; Wittinghofer, A. GEFs and GAPs: Critical Elements in the Control of Small G Proteins. *Cell* **2007**, *129* (5), 865-877.
(7) ten Klooster, J. P.; Hordijk, P. L. Targeting and localized signalling by small GTPases. *Biol. Cell* **2007**, *99* (1), 1-12.
(8) Resh, M. D. Covalent lipid modifications of proteins. *Curr. Biol.* **2013**, *23* (10), R431-435.
(9) Crosas-Molist, E.; Samain, R.; Kohlhammer, L.; Orgaz, J. L.; George, S. L.; Maiques, O.; Barcelo, J.; Sanz-Moreno, V. Rho GTPase signaling in cancer progression and dissemination. *Physiol. Rev.* **2022**, *102* (1), 455-510.
(10) Huang, L.; Guo, Z.; Wang, F.; Fu, L. KRAS mutation: from undruggable to druggable in cancer. *Signal Transduct. Target. Ther.* **2021**, *6* (1), 386.
(11) Narayanan, K. L.; Chopra, V.; Rosas, H. D.; Malarick, K.; Hersch, S. Rho Kinase Pathway Alterations in the Brain and Leukocytes in Huntington's Disease. *Mol. Neurobiol.* **2016**, *53* (4), 2132-2140.
(12) Aguilar, B. J.; Zhu, Y.; Lu, Q. Rho GTPases as therapeutic targets in Alzheimer's disease. *Alz. Res. Therapy* **2017**, *9* (1), 97.
(13) Kiral, F. R.; Kohrs, F. E.; Jin, E. J.; Hiesinger, P. R. Rab GTPases and Membrane Trafficking in Neurodegeneration. *Curr. Biol.* **2018**, *28* (8), R471-R486.
(14) Bei, Y.; Duong-Quy, S.; Hua-Huy, T.; Dao, P.; Le-Dong, N.-N.; Dinh-Xuan, A. T. Activation of RhoA/Rho-kinase pathway accounts for pulmonary endothelial dysfunction in patients with chronic obstructive pulmonary disease. *Physiol. Rep.* **2013**, *1* (5).
(15) Etzion, S.; Etzion, Y.; DeBosch, B.; Crawford, P. A.; Muslin, A. J. Akt2 deficiency promotes cardiac induction of Rab4a and myocardial β-adrenergic hypersensitivity. *J. Mol. Cell. Cardiol.* **2010**, *49* (6), 931-940.
(16) Filipeanu, C. M.; Zhou, F.; Lam, M. L.; Kerut, K. E.; Claycomb, W. C.; Wu, G. Enhancement of the Recycling and Activation of β-Adrenergic Receptor by Rab4 GTPase in Cardiac Myocytes*. *J. Biol. Chem.* **2006**, *281* (16), 11097-11103.
(17) Krzewski, K.; Cullinane, A. R. Evidence for defective Rab GTPase-dependent cargo traffic in immune disorders. *Exp. Cell. Res.* **2013**, *319* (15), 2360-2367.
(18) Burbage, M.; Keppler, S. J.; Gasparrini, F.; Martínez-Martín, N.; Gaya, M.; Feest, C.; Domart, M.-C.; Brakebusch, C.; Collinson, L.; Bruckbauer, A.; et al. Cdc42 is a key regulator of B cell differentiation and is required for antiviral humoral immunity. *J. Exp. Med.* **2014**, *212* (1), 53-72.
(19) Ambruso, D. R.; Knall, C.; Abell, A. N.; Panepinto, J.; Kurkchubasche, A.; Thurman, G.; Gonzalez-Aller, C.; Hiester, A.; deBoer, M.; Harbeck, R. J.; et al. Human neutrophil immunodeficiency syndrome is associated with an inhibitory Rac2 mutation. *Proc. Natl. Acad. Sci. U. S. A.* **2000**, *97* (9), 4654-4659.
(20) Ryan, M. B.; Fece de la Cruz, F.; Phat, S.; Myers, D. T.; Wong, E.; Shahzade, H. A.; Hong, C. B.; Corcoran, R. B. Vertical Pathway Inhibition Overcomes Adaptive Feedback Resistance to KRASG12C Inhibition. *Clin. Cancer Res.* **2020**, *26* (7), 1633-1643.
(21) Zhang, J. Z.; Ong, S.-E.; Baker, D.; Maly, D. J. Single-cell sensor analyses reveal signaling programs enabling Ras-G12C drug resistance. *Nat. Chem. Biol.* **2025**, *21* (1), 47-58.
(22) Chang, E. H.; Gonda, M. A.; Ellis, R. W.; Scolnick, E. M.; Lowy, D. R. Human genome contains four genes homologous to transforming genes of Harvey and Kirsten murine sarcoma viruses. *Proc. Natl. Acad. Sci. U. S. A.* **1982**, *79* (16), 4848-4852.
(23) John, J.; Sohmen, R.; Feuerstein, J.; Linke, R.; Wittinghofer, A.; Goody, R. S. Kinetics of interaction of nucleotides with nucleotide-free H-ras p21. *Biochemistry* **1990**, *29* (25), 6058-6065.

(24) Ostrem, J. M.; Peters, U.; Sos, M. L.; Wells, J. A.; Shokat, K. M. K-Ras(G12C) inhibitors allosterically control GTP affinity and effector interactions. *Nature* **2013**, *503* (7477), 548-551.
(25) Ostrem, J. M. L.; Shokat, K. M. Direct small-molecule inhibitors of KRAS: from structural insights to mechanism-based design. *Nat. Rev. Drug Discov.* **2016**, *15* (11), 771-785.
(26) Wang, X.; Allen, S.; Blake, J. F.; Bowcut, V.; Briere, D. M.; Calinisan, A.; Dahlke, J. R.; Fell, J. B.; Fischer, J. P.; Gunn, R. J.; et al. Identification of MRTX1133, a Noncovalent, Potent, and Selective KRASG12D Inhibitor. *J. Med. Chem.* **2022**, *65* (4), 3123-3133.
(27) Zheng, Q.; Zhang, Z.; Guiley, K. Z.; Shokat, K. M. Strain-release alkylation of Asp12 enables mutant selective targeting of K-Ras-G12D. *Nat. Chem. Biol.* **2024**, *20* (9), 1114-1122.
(28) Zhang, Z.; Guiley, K. Z.; Shokat, K. M. Chemical acylation of an acquired serine suppresses oncogenic signaling of K-Ras(G12S). *Nat. Chem. Biol.* **2022**, *18* (11), 1177-1183.
(29) Zhang, Z.; Morstein, J.; Ecker, A. K.; Guiley, K. Z.; Shokat, K. M. Chemoselective Covalent Modification of K-Ras(G12R) with a Small Molecule Electrophile. *J. Am. Chem. Soc.* **2022**, *144* (35), 15916-15921.
(30) Goreshnik, I.; Maly, D. J. A Small Molecule-Regulated Guanine Nucleotide Exchange Factor. *J. Am. Chem. Soc.* **2010**, *132* (3), 938-940.
(31) Rose, J. C.; Huang, P. S.; Camp, N. D.; Ye, J.; Leidal, A. M.; Goreshnik, I.; Trevillian, B. M.; Dickinson, M. S.; Cunningham-Bryant, D.; Debnath, J.; et al. A computationally engineered RAS rheostat reveals RAS-ERK signaling dynamics. *Nat. Chem. Biol.* **2017**, *13* (1), 119-126.
(32) Rose, J. C.; Dieter, E. M.; Cunningham-Bryant, D.; Maly, D. J. "Examining RAS pathway rewiring with a chemically inducible activator of RAS". *Small GTPases* **2020**, *11* (6), 413-420.
(33) Cunningham-Bryant, D.; Dieter, E. M.; Foight, G. W.; Rose, J. C.; Loutey, D. E.; Maly, D. J. A Chemically Disrupted Proximity System for Controlling Dynamic Cellular Processes. *J. Am. Chem. Soc.* **2019**, *141* (8), 3352-3355.
(34) Wu, Y. I.; Frey, D.; Lungu, O. I.; Jaehrig, A.; Schlichting, I.; Kuhlman, B.; Hahn, K. M. A genetically encoded photoactivatable Rac controls the motility of living cells. *Nature* **2009**, *461* (7260), 104-108.
(35) Wang, H.; Vilela, M.; Winkler, A.; Tarnawski, M.; Schlichting, I.; Yumerefendi, H.; Kuhlman, B.; Liu, R.; Danuser, G.; Hahn, K. M. LOVTRAP: an optogenetic system for photoinduced protein dissociation. *Nat. Methods* **2016**, *13* (9), 755-758.
(36) Toettcher, Jared E.; Weiner, Orion D.; Lim, Wendell A. Using Optogenetics to Interrogate the Dynamic Control of Signal Transmission by the Ras/Erk Module. *Cell* **2013**, *155* (6), 1422-1434.
(37) Johnson, H. E.; Goyal, Y.; Pannucci, N. L.; Schüpbach, T.; Shvartsman, S. Y.; Toettcher, J. E. The Spatiotemporal Limits of Developmental Erk Signaling. *Dev. Cell* **2017**, *40* (2), 185-192.
(38) Goglia, A. G.; Wilson, M. Z.; Jena, S. G.; Silbert, J.; Basta, L. P.; Devenport, D.; Toettcher, J. E. A Live-Cell Screen for Altered Erk Dynamics Reveals Principles of Proliferative Control. *Cell Syst.* **2020**, *10* (3), 240-253.e246.
(39) He, Y.; Faulkner, B. M.; Roberti, M. A.; Bassford, D. K.; Stains, C. I. Standardized Parts for Activation of Small GTPase Signaling in Living Cells. *Angew. Chem. Int. Ed.* **2024**, e202403499.
(40) He, Y.; Faulkner, B. M.; Weatherford, R.S.; Hyun, E.; Stains, C. I. Split-Small GTPase Reassembly as a Method to Control Cellular Signaling with User-Defined Inputs. *ACS Chem. Biol.* **2025**, *In Press,* DOI: 10.1021/acschembio.5c00083.
(41) Zhao, J.; Stains, C. I. Identification of a fragmented small GTPase capable of conditional effector binding. *RSC Adv.* **2017**, *7* (20), 12265-12268.
(42) Deisseroth, K. Optogenetics. *Nat. Methods* **2011**, *8* (1), 26-29.
(43) Arrenberg, A. B.; Stainier, D. Y. R.; Baier, H.; Huisken, J. Optogenetic Control of Cardiac Function. *Science* **2010**, *330* (6006), 971-974.
(44) Chang, K.-Y.; Woo, D.; Jung, H.; Lee, S.; Kim, S.; Won, J.; Kyung, T.; Park, H.; Kim, N.; Yang, H. W.; et al. Light-inducible receptor tyrosine kinases that regulate neurotrophin signalling. *Nat. Comm.* **2014**, *5* (1), 4057.
(45) Tkatch, T.; Greotti, E.; Baranauskas, G.; Pendin, D.; Roy, S.; Nita, L. I.; Wettmarshausen, J.; Prigge, M.; Yizhar, O.; Shirihai, O. S.; et al. Optogenetic control of mitochondrial metabolism and Ca2+ signaling by mitochondria-targeted opsins. *Proc. Natl. Acad. Sci. U. S. A.* **2017**, *114* (26), E5167-E5176.
(46) Yu, D.; Lee, H.; Hong, J.; Jung, H.; Jo, Y.; Oh, B.-H.; Park, B. O.; Heo, W. D. Optogenetic activation of intracellular antibodies for direct modulation of endogenous proteins. *Nat. Methods* **2019**, *16* (11), 1095-1100.

(47) Huang, Z.; Wu, Y.; Allen, M. E.; Pan, Y.; Kyriakakis, P.; Lu, S.; Chang, Y.-J.; Wang, X.; Chien, S.; Wang, Y. Engineering light-controllable CAR T cells for cancer immunotherapy. *Sci. Adv.* **2020**, *6* (8), eaay9209.
(48) Mashita, T.; Kowada, T.; Yamamoto, H.; Hamaguchi, S.; Sato, T.; Matsui, T.; Mizukami, S. Quantitative control of subcellular protein localization with a photochromic dimerizer. *Nat. Chem. Biol.* **2024**, *20* (11), 1461-1470.
(49) Ong, Q.; Lim, L. T. R.; Goh, C.; Liao, Y.; Chan, S. E.; Lim, C. J. Y.; Kam, V.; Yap, J.; Tseng, T.; Desrouleaux, R.; et al. Spatiotemporal control of subcellular O-GlcNAc signaling using Opto-OGT. *Nat. Chem. Biol.* **2025**, *21* (2), 300-308.
(50) Crefcoeur, R. P.; Yin, R.; Ulm, R.; Halazonetis, T. D. Ultraviolet-B-mediated induction of protein–protein interactions in mammalian cells. *Nat. Comm.* **2013**, *4* (1), 1779.
(51) Christie, J. M.; Reymond, P.; Powell, G. K.; Bernasconi, P.; Raibekas, A. A.; Liscum, E.; Briggs, W. R. Arabidopsis NPH1: A Flavoprotein with the Properties of a Photoreceptor for Phototropism. *Science* **1998**, *282* (5394), 1698-1701.
(52) Kennedy, M. J.; Hughes, R. M.; Peteya, L. A.; Schwartz, J. W.; Ehlers, M. D.; Tucker, C. L. Rapid blue-light–mediated induction of protein interactions in living cells. *Nat. Methods* **2010**, *7* (12), 973-975.
(53) Kainrath, S.; Stadler, M.; Reichhart, E.; Distel, M.; Janovjak, H. Green-Light-Induced Inactivation of Receptor Signaling Using Cobalamin-Binding Domains. *Angew. Chem. Int. Ed.* **2017**, *56* (16), 4608-4611.
(54) Chatelle, C.; Ochoa-Fernandez, R.; Engesser, R.; Schneider, N.; Beyer, H. M.; Jones, A. R.; Timmer, J.; Zurbriggen, M. D.; Weber, W. A Green-Light-Responsive System for the Control of Transgene Expression in Mammalian and Plant Cells. *ACS Synth. Biol.* **2018**, *7* (5), 1349-1358.
(55) Redchuk, T. A.; Omelina, E. S.; Chernov, K. G.; Verkhusha, V. V. Near-infrared optogenetic pair for protein regulation and spectral multiplexing. *Nat. Chem. Biol.* **2017**, *13* (6), 633-639.
(56) Zhou, Y.; Kong, D.; Wang, X.; Yu, G.; Wu, X.; Guan, N.; Weber, W.; Ye, H. A small and highly sensitive red/far-red optogenetic switch for applications in mammals. *Nat. Biotechnol.* **2022**, *40* (2), 262-272.
(57) Guntas, G.; Hallett, R. A.; Zimmerman, S. P.; Williams, T.; Yumerefendi, H.; Bear, J. E.; Kuhlman, B. Engineering an improved light-induced dimer (iLID) for controlling the localization and activity of signaling proteins. *Proc. Natl. Acad. Sci. U. S. A.* **2015**, *112* (1), 112-117.
(58) Zimmerman, S. P.; Hallett, R. A.; Bourke, A. M.; Bear, J. E.; Kennedy, M. J.; Kuhlman, B. Tuning the Binding Affinities and Reversion Kinetics of a Light Inducible Dimer Allows Control of Transmembrane Protein Localization. *Biochemistry* **2016**, *55* (37), 5264-5271.
(59) Crosson, S.; Moffat, K. Structure of a flavin-binding plant photoreceptor domain: Insights into light-mediated signal transduction. *Proc. Natl. Acad. Sci. U. S. A.* **2001**, *98* (6), 2995-3000.
(60) Rohatgi, R.; Ma, L.; Miki, H.; Lopez, M.; Kirchhausen, T.; Takenawa, T.; Kirschner, M. W. The Interaction between N-WASP and the Arp2/3 Complex Links Cdc42-Dependent Signals to Actin Assembly. *Cell* **1999**, *97* (2), 221-231.
(61) Mattila, P. K.; Lappalainen, P. Filopodia: molecular architecture and cellular functions. *Nat. Rev. Mol. Cell Biol.* **2008**, *9* (6), 446-454.
(62) Bagci, H.; Sriskandarajah, N.; Robert, A.; Boulais, J.; Elkholi, I. E.; Tran, V.; Lin, Z.-Y.; Thibault, M.-P.; Dubé, N.; Faubert, D.; et al. Mapping the proximity interaction network of the Rho-family GTPases reveals signalling pathways and regulatory mechanisms. *Nat. Cell Biol.* **2020**, *22* (1), 120-134.
(63) Tojkander, S.; Gateva, G.; Lappalainen, P. Actin stress fibers – assembly, dynamics and biological roles. *J. Cell Sci.* **2012**, *125* (8), 1855-1864.
(64) Takano, T.; Wu, M.; Nakamuta, S.; Naoki, H.; Ishizawa, N.; Namba, T.; Watanabe, T.; Xu, C.; Hamaguchi, T.; Yura, Y.; et al. Discovery of long-range inhibitory signaling to ensure single axon formation. *Nat. Comm.* **2017**, *8* (1), 33.
(65) Mori, K.; Amano, M.; Takefuji, M.; Kato, K.; Morita, Y.; Nishioka, T.; Matsuura, Y.; Murohara, T.; Kaibuchi, K. Rho-kinase Contributes to Sustained RhoA Activation through Phosphorylation of p190A RhoGAP*. *J. Biol. Chem.* **2009**, *284* (8), 5067-5076.
(66) Vega, F. M.; Fruhwirth, G.; Ng, T.; Ridley, A. J. RhoA and RhoC have distinct roles in migration and invasion by acting through different targets. *J. Cell Biol.* **2011**, *193* (4), 655-665.
(67) Takenawa, T.; Suetsugu, S. The WASP–WAVE protein network: connecting the membrane to the cytoskeleton. *Nat. Rev. Mol. Cell Biol.* **2007**, *8* (1), 37-48.

(68) Hallett, R. A.; Zimmerman, S. P.; Yumerefendi, H.; Bear, J. E.; Kuhlman, B. Correlating in Vitro and in Vivo Activities of Light-Inducible Dimers: A Cellular Optogenetics Guide. *ACS Synth. Biol.* **2016**, *5* (1), 53-64.
(69) Jacquemet, G.; Hamidi, H.; Ivaska, J. Filopodia Quantification Using FiloQuant. In *Computer Optimized Microscopy: Methods and Protocols*, Rebollo, E., Bosch, M. Eds.; Springer New York, 2019; pp 359-373.